Three-Dimensional Contrasted Visualization of Pancreas in Rats Using Clinical MRI and CT Scanners

Journal:	*Contrast Media and Molecular Imaging*
Manuscript ID:	CMMI-14-0059.R1
Wiley - Manuscript type:	Full Paper
Date Submitted by the Author:	n/a
Complete List of Authors:	YIN, TING; Theragnostic Laboratory, Department of Imaging & Pathology Coudyzer, Walter; University Hospital Gauthuisberg, Department of Radiology Peeters, Ronald; University Hospital Gauthuisberg, Department of Radiology Liu, Yewei; Theragnostic Laboratory, Department of Imaging & Pathology Cona, Marlein; Theragnostic Laboratory, Department of Imaging & Pathology Feng, Yuanbo; Theragnostic Laboratory, Department of Imaging & Pathology Xia, Qian; Theragnostic Laboratory, Department of Imaging & Pathology Yu, Jie; University Hospital Gauthuisberg, Department of Radiology Jiang, Yansheng; Theragnostic Laboratory, Department of Imaging & Pathology Dymarkowski, Steven; University Hospital Gauthuisberg, Department of Radiology Huang, Gang; Shanghai Jiaotong University, Department of Nuclear Medicine Chen, Feng; Zhejiang University, the First Affiliated Hospital, Department of Radiology Oyen, Raymond; University Hospital Gauthuisberg, Department of Radiology Ni, Yicheng; Theragnostic Laboratory, Department of Imaging & Pathology; University Hospital Gauthuisberg, Department of Radiology
Keyword:	contrast enhanced imaging, rat pancreas, image processing, 3D visualization

Three-Dimensional Contrasted Visualization of Pancreas in Rats Using Clinical MRI and CT Scanners

Ting Yin, MSc[1]; Walter Coudyzer, MSc[2]; Ronald Peeters, PhD[2]; Yewei Liu, MD[1,3]; Marlein Miranda Cona, PhD[1]; Yuanbo Feng, MD, PhD[1,2]; Qian Xia, MD, PhD[1,3]; Jie Yu, MD[1,2]; Yansheng Jiang, PhD[1,2]; Steven Dymarkowski, MD, PhD[2]; Gang Huang, MD, PhD[3]; Feng Chen, MD, PhD[1,4]; Raymond Oyen, MD, PhD[2]; Yicheng Ni, MD, PhD[1,2*]

[1]Theragnostic Laboratory, Department of Imaging & Pathology, Biomedical Sciences Group, KU Leuven, Herestraat 49, 3000 Leuven, Belgium

[2]Department of Radiology, University Hospitals, KU Leuven, Herestraat 49, 3000 Leuven, Belgium

[3]Department of Nuclear Medicine, School of Medicine, Shanghai Jiaotong University, China

[4]Department of Radiology, the First Affiliated Hospital, Zhejiang University, China

[*]Corresponding author

Yicheng Ni MD, PhD

Department of Radiology, University Hospitals, KU Leuven, Herestraat 49, 3000 Leuven, Belgium

Email: yicheng.ni@med.kuleuven.be

Tel: +32 16 33 01 65

Fax: +32 16 34 37 65

Conflicts of interest and Source of Funding: The authors declare no conflict of interest. This study was partially supported by the grants awarded by the KU Leuven Molecular Small Animal Imaging Center MoSAIC (KUL EF/05/08) and KU Leuven the center of excellence In vivo Molecular Imaging Research (IMIR). The corresponding author Ni Y is currently a Bayer Lecture Chair holder.

Short title: Rat Pancreas on Contrasted MRI and CT

Abstract

Purpose: To visualize the pancreas in postmortem rats with local contrast medium infusion by three dimensional (3D) magnetic resonance imaging (MRI) and computed tomography (CT) using clinical imagers.

Methods: A total of 16 Sprague-Dawley rats about 300g were used for the pancreas visualization. Following the baseline imaging, a mixed contrast medium dye called Gadolodo-EB containing optimized concentrations of Gd-DOTA, Iomeprol and Evens blue was infused into the distally obstructed common bile duct (CBD) for postcontrast imaging at 3.0T MRI and 128-slice CT scanners. Images were post-processed with MeVisLab software package. MRI findings were co-registered with CT scans and validated with histomorphology, with relative contrast ratios quantified.

Results: Without contrast enhancement, the pancreas was indiscernible. After infusion of Gadolodo-EB solution, only pancreatic region became outstandingly visible, as shown by 3D rendering MRI and CT and proven by colored dissection and histological examinations. The measured volume of the pancreas averaged at 1.12±0.04cm^3 after standardization. Relative contrast ratios were 93.28±34.61% and 26.45±5.29% for MRI and CT respectively.

Conclusions: We have developed a multifunctional contrast medium dye to help clearly visualize and delineate rat pancreas *in situ* using clinical MRI and CT scanners. The topographic landmarks thus created with 3D demonstration may help to provide guidelines for the next *in vivo* pancreatic MR imaging research in rodents.

Key Words: contrast enhanced imaging, rat pancreas, image processing, 3D visualization

Introduction

Causative factors on the pancreas result in diseases such as pancreatitis, diabetes, and pancreatic tumors (1,2). The high incidence and mortality of pancreatic diseases have positioned imaging diagnosis a crucial place in daily clinical practice.

With the spatial and temporal resolution approaching that of computed tomography (CT), magnetic resonance imaging (MRI) has been increasingly utilized in clinic diagnosis of pancreatic lesions due to its additional advantages such as superb soft tissue contrast, ionizing-radiation free and multiparametric capacity (3,4). The combination of basic T1/T2 sequences, diffusion weighted imaging (DWI) and contrast enhanced MRI improves the accuracy of diagnosis for pancreatic tumors (5). The invention of MR cholangiopancreatography (MRCP) makes noninvasive examination of biliopancreatic duct system possible without any post-procedural complications (6,7).

In order to explore the mechanisms of pancreatic pathologies and develop new diagnostic and therapeutic techniques, rodent models are often used in pancreatic studies. However, unlike pancreas in humans, which is a retroperitoneal solid organ and can be identified by imaging even without contrast enhancement (3,8), rodent pancreas appears as an irregular lobulated organ, which is indiscernible compared to surrounding tissues, making imaging pancreas in rodents extremely challenging (9,10).

Efforts have been made in rodent pancreas MR imaging such as pancreatic islets imaging and pancreatic vessels permeability imaging using dynamic contrast enhanced MRI (11–13). However, due to the lack of pancreas specific labeling, pancreatic tissue in rodents itself is still very difficult to be distinguished from the surrounding structures such as caudate liver lobes, omenta and other peri-gastrointestinal soft tissues. Moreover, even after labeling, it is still challenging to have a complete overview of the entire pancreas due to the random movement of guts around pancreatic head portion. At this stage, the failure to image the entire pancreas has hampered our study on pancreatic diseases (e.g. acute pancreatitis), since nil or partial visualization of rodent pancreas could not reflect the overall pathological changes.

In this study, we intended to image rat pancreas *in situ* by using the state-of-the-art clinical MRI and CT scanners with the assistance of intra-pancreatic contrast enhancement. Detailed imaging landmarks and morphometry of rat pancreas were measured, described and presented with three dimensional (3D) rendering. Such postmortem investigation may help clearly recognize rat pancreas anatomy, provide a standard topography of this organ, and pave the way for the next *in vivo* 3D high resolution imaging studies on normal pancreas and pancreatic diseases in rat models.

Materials and methods

This experiment was approved by the ethical committee of our institute for animal research and welfare, and performed according to a designed protocol (Fig. 1).

Animals

Twelve Sprague-Dawley rats of equal genders weighing between 270 to 350g were subjected to both in vivo and postmortem imaging studies after being fasted for 6 hours prior to the experiments. Additional 4 rats of equal genders were used for dissection and histomorphological studies as normal controls.

Contrast solution preparation, characterization and administration

For multimodality contrasted imaging visualization of pancreas in rodents, phantoms with CT and MRI contrast agents at gradient concentrations and their dye mixtures were prepared and screened with CT and MRI. Consequently, a mixed hydrophilic solution called GadoIodo-EB containing 2 mM gadolinium contrast agent Gd-DOTA (Dotarem®, Guerbet, France) for MRI, Iomeprol (Iomeron®, Bracco, Italy) at 10 mg iodine/ml for CT and 0.1% Evans blue (EB, Sigma-Aldrich, USA) diluted in normal saline was optimized and made ready for instillation into the biliopancreatic duct at 0.6 ml per rat to demonstrate the pancreas by CT, MRI and visual inspection. Furthermore, such solutions of separate components or as a mixture GadoIodo-EB were characterized by high-performance liquid chromatography (UV-Vis HPLC detector 190-900 nm, Auckland, New Zealand) for testing their chemical stabilities.

In vivo MRI

MRI was performed at a 3.0T clinical scanner (Magnetom Tim Trio, Siemens, Erlangen, Germany). MR signal was transmitted through the 60 cm size bore body coil with maximum gradient amplitude of 45mT/m and slew rate of 200mT/m/ms, which was combined with an 8 channel phase array wrist coil as receiver. In vivo and postmortem MRI acquisition parameters are summarized in table 1. For in vivo MR scanning, animals were anesthetized by inhalation of 1 to 2 % isoflurane (mixed with oxygen and air) and placed in a supine position while images were acquired. MR compatible small animal physiological monitoring system (SAII, Stony Brook, NY, USA) was applied for respiration triggering. A 0.3 mm isotropic 3D gradient echo

flash low angle shot (FLASH) sequence with segmented k-space acquisition and a flow compensate T2 weighted 3D turbo spin-echo (TSE) with variable-flip-angle refocusing RF pulses (SPACE) sequence were performed.

Postmortem imaging acquisition

For preparing postmortem studies, rats were first anesthetized with intraperitoneal pentobarbital (Nembutal; Sanofi Sante Animale, Brussels, Belgium) at a dose of 40 mg/kg. After hair shaving and skin sterilization, a midline incision was made to expose the liver and other abdominal organs, particularly the hepatic portal area. To block the secretion pathway, the biliopancreatic duct was ligated in close vicinity to duodenal papilla, similarly to the technique mentioned in Kare's study (14). Afterwards, a 16 cm silicone catheter of 1.0 mm outer diameter (Degania Silicone Ltd, Degania Bet, 1513000, Israel) was inserted 6 mm deep into the common bile duct (CBD) near the hepatic port to the direction of duodenum for GadoIodo-EB infusion. The catheter was anchored with a 5-0 silk suture and connected to a 1.0 ml syringe loaded with the GadoIodo-EB contrast medium dye solution. After closure of abdominal incision by two layers of suture, the animal was euthanized by intravenous overdose of Nembutal to nullify imaging motion artifacts.

Following a baseline precontrast MRI scanning, pre- and postcontrast CT images were acquired on a clinic CT scanner (Somatom Definition Flash, Siemens, Erlangen, Germany) using low tube voltage of 80 kVp, total X-ray exposure time was 53s for each scan. High resolution transversal imaging was reconstructed and processed in Syngo CT 2012B with matrix size of 512*512, and a slice distance of 0.2 mm. Such 3D-CT scans allowed imaging rat abdomen on a relatively noise-free background to validate the presence of contrast agent in the pancreas (see video-supplement 1).

Postmortem MRI with 3D FLASH sequence was performed to evaluate the T1 enhancement by Gd-DOTA with isotropic spatial resolution of 0.3 mm, SPACE sequence was applied to acquire high-resolution anatomical information for rat abdomen, and ultra-short echo time (UTE) sequence was used to highlight tissues with short T2 in abdomen. Such 3D MRI scans enabled not only pancreas depiction but also neighboring organ localization (see video-supplement 2).

Image processing

All imaging analyses and visualizations were accomplished in MeVisLab platform (www.mevislab.de). CT images were co-registered to MRI space using MeVis Image Registration Toolkit (MERIT), in which affine transformation using normalized mutual information similarity measurements was applied. Afterwards, contrast enhanced pancreas was segmented from subtracted T1-weighted MR imaging and resampled CT imaging using fuzzy c-mean spatial classification algorithm with a proper intensity threshold, followed by region growing approach with 3D-6 nearest neighbor search. Segmented pancreas tissue volume was measured automatically.

Fat distribution in rat abdomen was delineated by subtracting SPACE scans with and without spectral fat saturation. Organs surrounding the pancreas were manually contoured or segmented semi-automatically from UTE or SPACE images only for 3D demonstration of pancreatic topography. Resampled pre-contrast CT bone image was used as background scaffold.

Tissue preparation and histology

After acquiring all images, animals were reopened to harvest the pancreas organ guided by Gadolodo-EB coloration. Dissection was made along the boundaries of the blue dye stained pancreatic tissues. The pancreas was cleaned from fat tissue and actual pancreatic volume was measured by immersing tissue into distilled water within a metering tank. Tissue was fixed in 10% formalin and embedded for paraffin sections. Afterwards, 5 μm thickness slices were stained with hematoxylin and eosin (HE) for optical microscopic assessment (Axioskop, Zeiss, Oberkoche, Germany) and digital photography to compare pancreatic tissues without and with contrast injection.

Image quality assessment

Signal intensity (SI) was measured within the pancreatic region, and contrast ratio (CR) after Gadolodo-EB infusion was calculated by the following equation: CR = [SI(post)-SI(pre)]/SI(pre)*100%. Visibility of the pancreas, splenic vein and CBD on both MRI and CT were assessed and summarized.

Results

General aspects

All experimental procedures were carried out smoothly according to the pre-designed protocol (Fig. 1) without accidental loss of animals. The clinical CT and MRI imagers were adapted well for the purpose of the present study in rats. No apparent variation of the pancreas was observed between male and female rats, although a movable kidney and an extra rib on the right were encountered in two individual rats as anatomical variations among this population.

Contrast agent solution characterization

A representative UV chromatogram of mixed contrast medium dye GadoIodo-EB consisting of 2.0 mM Gd-DOTA, 10mg Iodine/ml Iomeprol and 0.1% Evans blue dye is shown in Figure 2. The profiles clearly revealed only two peaks whose retention times (RTs) perfectly matched with those observed by analyzing separate standard solutions of Iomeprol and Evans blue dye (data not shown). The sharp peak corresponded to the CT agent Iomeprol with a RT of 1.80±0.01 min. The second broad peak with a RT of 5.99±0.02 min referred to Evans blue. Neither in the standard solution nor in the mixture of Gadolodo-EB could Gd-DOTA be detected due to its structural lack of UV chromospheres for the HPLC technique applied. However, both peaks of Iomeprol and Evans blue in the mixture were not altered by adding Gd-DOTA, of which the presence was affirmed by the MRI studies, indicating that no chemical reactions occurred within the mixture of Gadolodo-EB. Phantom studies showed that neither the presence of Gd-DOTA on CT nor Iomeprol on MRI changed intrinsic signal intensity of the contrast medium dye at their concentrations applied.

In vivo MRI

Three dimensional high resolution in vivo MRI without contrast enhancement displayed abdominal anatomy that could be useful for searching pancreas-related landmarks such as the CBD or biliopancreatic duct and splenic vein. For examples, on 3D T2 SPACE image, the CBD and its extending biliopancreatic duct appeared with a strong hyperintensity (Fig. 3a, table 2) and hypointense splenic vein was

shown in full length, which likely goes along with pancreatic body and tail (Fig. 3b, table 2), as revealed by later contrasted postmortem studies.

Contrast enhanced MRI

Pre- and postcontrast T1 and T2 MRI images are shown with the same anatomic positions. On T1 FLASH image, before contrast infusion, there was no difference of signal intensities between the pancreas and surrounding organs (Fig. 3c, table 2). After GadoIodo-EB infusion, pancreatic region appeared hyperintense, indicating the T1-shortening effect of the gadolinium chelate (Fig. 3d, table 2). On T2 SPACE images, the pancreas was virtually invisible (Fig. 3c'). But, hyperintense signal intensity appeared after GadoIodo-EB infusion due to the presence of saline solvent or long-T2 water (Fig. 3d'), because the low-concentrated Gd-DOTA had negligible T2--shortening effects.

CT findings

Before contrast instillation, the pancreas was invisible when image density was set to a threshold value for bone visualization by experienced radiologists (Fig. 4a, 4b). But, the infused GadoIodo-EB provided a clear contrast for pancreas alone, displaying it as an outstanding organ in abdomen (Fig. 4a', b'). In addition to the pancreas, hyperdense subjects also existed in the abdominal region on pre-contrast CT scan, which were proven as calcified food residues within the fecal pellets located in large intestines (Fig. 4b, b' and video supplements).

Topographic descriptions

As shown by postmortem contrasted CT and MRI scans in this study (Fig. 3-5), the entire pancreas in rats appears as a "T" shaped structure, but tilted 90° to the right, with the short vertical bar (pancreatic head) at least 2 times thicker than the long horizontal bar (pancreatic body and tail). The entire rat pancreas locates in the upper abdomen at the level either between the 11^{th} thoracic vertebra (T11) and the 2^{nd} lumbar vertebra (L2) or between the T12 and L3 with slight individual variations (Fig. 5b, b' and video supplements). Similar to that of humans, though not in the same proportions, the pancreas in rats can be divided into pancreatic head, body and tail. The head is further divided into the biliary portion located along the CBD on the right side of portal vein and gastric pylorus, and the duodenal portion largely enclosed by

the “C” shaped duodenum to the left of the right kidney. The pancreatic body and tail form a horizontal entity that is also called gastrosplenic portion located inferior to the stomach to the right of the spleen (14) and left kidney (video supplements).

Contrasted topography of rat pancreas imaging enabled recognizing a few landmarks that may help position the pancreas in rats *in vivo* as described below:

1) a 2-cm elongation line from the CBD downwards can be referred as a landmark for localizing pancreatic head anterior to the hilum of the right kidney and largely wrapped by the duodenal loop (Fig. 3a, 5b’);

2) pancreatic body and tail locate inferoposterior to the stomach and caudate lobes of the liver and adjacent to the anterosuperior part of the left kidney (Fig. 5a, a’);

3) the entire splenic vein joining to the portal vein goes along with pancreatic body and tail to the right of the spleen and in front of the left kidney (Fig. 3b, c, c’).

Their relative positions are illustrated by color-coded imaging extraction (Fig. 5b’). Fat tissues can be confused with the pancreas, which could be differentiated by highlighting the fat (in purple color) using fat saturated SPACE images (Fig. 5a, a’). Segmented pancreas and its landmarks were shown by 3D rending images using the bony thorax as a background scaffold (Fig. 5b, b’ and video supplement 2).

Dissection and histology

Under a re-laparotomy for *ex vivo* examinations, digital photos showed Evans blue staining of pancreatic tissues (Fig. 6a). Microscopically, pancreatic exocrine tissue, expanded pancreatic duct and endocrine islets of Langerhans were identified with H&E stained histology. Except slightly dilated exocrine glandular system, there was no significant difference between contrast-infused and control pancreases (Fig. 6b, c).

Quantitative measurements

After adjusted normalization, pancreatic volumes measured by imaging and *ex vivo* analysis were 1.12 ± 0.04 cm^3 and 1.17 ± 0.10 cm^3 respectively, which is in line with the pancreas weight about 1.2 g for SD rats ranging from 270 to 450 g of body weight as reported by a previous study (15). The relative contrast ratio for post-contrast FLASH-MRI and CT images was enhanced by 93.28 ± 34.61 % and 26.45 ± 5.29 % respectively compared to pre-contrast images (table 2).

Discussion

One bottleneck of research on pancreatic disorders in rodents is the virtual inability to noninvasively detect the lesion on this organ, to monitor the disease progress and to follow up the therapies by imaging modalities, which has hampered advances in the field. As the first step in our serial efforts, we attempted to visualize rat pancreas postmortem by contrast enhanced MRI and CT using clinically available imagers. To the best of our knowledge, it is the first time that the in situ rodent pancreas is so clearly depicted in terms of its location, dimension, contour and relations to the adjacent anatomical structures, which may provide useful clues or landmarks for identifying rat pancreas and its pathologies during further in vivo pancreatic imaging research.

Currently, CT is still the most commonly used imaging modality for diagnosis of pancreatitis and pancreatic tumors due to its temporal efficiency and unbiased contrast compared to MRI (16,17). Therefore, we applied CT for cross-reference to our MRI findings.

The utilization of the clinical MRI and CT scanners in combination with the FDA approved contrast agents would make our findings more clinically translational. It also demonstrates that clinicians in academic institutes could perform preclinical animal experiments without relying on the dedicated equipment for small animals. Since the achievable spatial resolution could be limited in comparison to the miniaturized animal imagers, certain technical optimization was necessary particularly for imaging rat pancreas as a tiny irregular abdominal organ.

Accordingly, we adapted higher resolution 3D scanning protocols to include as many details as possible, though such 3D scans were more time-consuming with higher imaging noise relative to 2D scans. In this study, both T1 weighted FLASH and T2 weighted SPACE protocols were applied for contrasted and structural evaluations respectively. Results showed that without regional contrast agent instillation, it was impossible to distinguish rodent pancreas from the surrounding tissues through those imaging protocols.

Because a real pancreas-specific contrast agent does not exist, in this study we prepared a mixed water-soluble solution GadoIodo-EB that consists of two extracellular water-soluble contrast agents, Gd-DOTA for MRI and Iomeprol for CT

(18,19) both of which do not undergo intracellular uptake, and a blue dye. Once infused, the solution with optimized concentrations of gadolinium and iodine was filled into the exocrine glandular system, leading to the striking contrast observed only in the pancreas on both MRI and CT scans. The postcontrast inhomogeneity of MRI signal within the pancreas reflects such intraorganal distribution pattern of Gd-DOTA as also evidenced on colored dissection. The mixture of these two contrast agents with Evans blue dye did not alter their chemical properties as proven by HPLC. Since all these 3 components are nontoxic and intravenously injectable in humans, and since imaging and HPLC outcomes in our study have implied their inert chemical properties while mixed, GadoIodo-EB as a multifunctional diagnostic agent could be combined with interventional procedures e.g. endoscopic retrograde cholangiopancreatography (ERCP) and laparoscopic cholecystectomy, etc. for multimodality imaging diagnosis and/or intraoperative optical imaging observation. Such potential clinical applications warrant further experimental investigations.

Without local contrast instillation, the pancreas shows the same signal intensity or tissue density as the liver does. Thus hepatic caudate lobe, which locates closely next to the pancreatic body, could be mistaken as the pancreas in the literature (20). Indeed, the pancreas shares similar soft tissue imaging features with other abdominal organs on both MRI and CT, even after systematical contrast agent administration. Therefore, it is essential to track the pancreas in vivo by carefully navigating through certain landmarks including adjacent organs and important vessels on 3D images. Thus, guided by the artificially contrasted pancreas in this study, we were able to identify a few such useful landmarks including the CBD, splenic vein, caudate liver lobes, the stomach, the duodenum, the right and left kidney and the spleen, which together make the in-between contour of pancreas. Abdominal fat tissues in rats especially those adhered to the pancreas could be distinguished by using fat-saturation MRI sequences. However, omentum tissues appeared more difficult to identify, which could only be recognized on histology.

MRI is known to be superior to CT in soft tissue contrast, but the plain scans of both modalities proved insufficient to visualize rodent pancreas, and the use of contrast agents was deemed necessary. For this, two obstacles should be tackled. First, since pancreas-specific contrast agents do not exist, we had to use commercially available nonspecific ones such as Gd-DOTA and Iomeprol for MRI and CT respectively. They

are made for intravenous injection at a high concentration. After administration they undergo extracellular distribution without intracellular uptake, and tissues or organs are properly enhanced by them at much diluted concentrations. If without dilution, the presence of CT or MRI contrast agents at their original concentrations (0.5M for Gd-DOTA and 300mg Iodine/ml for Iomeprol) in the scanned volume would cause strong artifacts that would mask the authentic images. This was the reason why we had to perform in vitro tests first to optimize the mixed contrast dye Gadolodo-EB for the appropriate concentrations of both Gd-DOTA and Iomeprol. Secondly, the presence of such a contrast dye had to be confined only in the pancreas but not elsewhere to selectively enhance this organ on both CT and MR images. To do so, we took advantage of the biliopancreatic anatomy in rats and filled the pancreatic exocrine ductal system entirely with Gadolodo-EB so that only the pancreas could be outstandingly enhanced on both CT and MRI.

In order to avoid blooming effect while maintaining adequate contrast enhancement, the concentration of each contrast agent used in this study was optimized to a clinically acceptable range. The total volume of Gadolodo-EB for infusion into the pancreas was also controlled to less than the total volume of pancreas.

There were rodent pancreatic imaging using micro-CT (9), and specific pancreatic labeling using high-resolution SPECT technique (21). Contrast enhanced MRI suffered from motion artifact due to the special location of pancreas (22). As observed by both imaging and histology, pancreatic head was closely surrounded by duodenum and attached to the large intestine, where the wave movement was unpredictable and cannot be monitored, which leads to blurring artifact of the entire region. Therefore, fasting is preferred prior to in vivo imaging to reduce gut movements. Besides, fasting for 6 hours leaves more upper abdominal space for Gadolodo-EB infusion and eases surgical operation. More specific enhancement on inflamed pancreas (23) or pancreatic islets surface reporter (24) may help improve the imaging accuracy on the pancreas, however such specific contrast agents are still unavailable.

From our in vivo observations, without contrast enhancement, the CBD showed prominent hyperintense on SPACE images. Pancreatic ducts, on the other hand, were difficult to highlight due to the limited spatial resolution. Although there are

abundant blood supplies to the pancreas, only the splenic vein was thick enough to be observed by our imaging sequences. Therefore, it seems also essential for in vivo pancreas imaging to apply a contrast agent, ideally a pancreas-specific one.

In conclusion, visualization of a complete pancreas was achieved through contrast enhanced CT and MRI imaging in a novel rat postmortem model. Detailed pancreatic landmarks were thus described and demonstrated with 3D rendering, including the depicted CBD and splenic vein on in vivo images. To identify other in vivo features of rodent pancreas, contrast enhanced protocols will be elaborated in the future.

References

1. Nakamura T, Takeuchi T, Tando Y. Pancreatic dysfunction and treatment options. Pancreas 1998;16:329–36.

2. Cascinu S, Falconi M, Valentini V, Jelic S. Pancreatic cancer: ESMO Clinical Practice Guidelines for diagnosis, treatment and follow-up. Ann. Oncol. 2010;21:55–58. doi: 10.1093/annonc/mdq165.

3. Sandrasegaran K, Lin C, Akisik FM, Tann M. State-of-the-art pancreatic MRI. Am. J. Roentgenol. 2010;195:42–53. doi: 10.2214/ajr.195.3_supplement.0s42.

4. Chaudhary V, Bano S. Imaging of the pancreas: Recent advances. Indian J. Endocrinol. Metab. 2011;15:S25–32. doi: 10.4103/2230-8210.83060.

5. Schima W. MRI of the pancreas: tumours and tumour-simulating processes. Cancer Imaging 2006;6:199–203. doi: 10.1102/1470-7330.2006.0035.

6. Fulcher AS, Turner MA. MR pancreatography: a useful tool for evaluating pancreatic disorders. Radiographics 1998;19:5–24. doi: 10.1148/radiographics.19.1.g99ja045.

7. Nandalur KR, Hussain HK, Weadock WJ, Wamsteker EJ, Johnson TD, Khan AS, D'Amico AR, Ford MK, Nandalur SR, Chenevert TL. Possible biliary disease: diagnostic performance of high-spatial-resolution isotropic 3D T2-weighted MRCP. Radiology 2008;249:883–90. doi: 10.1148/radiol.2493080389.

8. Sainani N, Catalano O, Sahani D. Pancreas. In: John R. Haaga, Vikram S. Dogra, Michael Forsting E, editor. CT and MRI of the Whole Body. 5th ed. Elsevier; 2002.

9. Akladios CY, Bour G, Raykov Z, Mutter D, Marescaux J AM. Structural imaging of the pancreas in rat using micro-CT: application to a non-invasive longitudinal evaluation of pancreatic ductal carcinoma monitoring. J Cancer Res Ther 2013;1:70–76.

10. Tchokonte-Nana V, Longo-Mbenza B, Page BJ, Du Toit DF. Morphogenetic and clinical perspectives on the neogenesis of pancreatic duct ligation-induced islet cells : a review. Adv Clin Exp Med [Internet] 2011;20:5–14.

11. Lamprianou S, Immonen R, Nabuurs C, Gjinovci A, Vinet L, Montet XCR, Gruetter R, Meda P. High-resolution magnetic resonance imaging quantitatively detects individual pancreatic islets. Diabetes 2011;60:2853–60. doi: 10.2337/db11-0726.

12. Medarova Z, Greiner DL, Ifediba M, Dai G, Bolotin E, Castillo G, Bogdanov A, Kumar M, Moore A. Imaging the pancreatic vasculature in diabetes models. Diabetes. Metab. Res. Rev. 2011;27:767–72. doi: 10.1002/dmrr.1249.

13. Medarova Z, Castillo G, Dai G, Bolotin E, Bogdanov A, Moore A. Noninvasive magnetic resonance imaging of microvascular changes in type 1 diabetes. Diabetes 2007;56:2677–82. doi: 10.2337/db07-0822.

14. Kara ME. The anatomical study on the rat pancreas and its ducts with emphasis on the surgical approach. Ann. Anat. 2005;187:105–12. doi: 10.1016/j.aanat.2004.10.004.

15. Montanya E, Nacher V, Soler, Joan E. Linear Correlation Between beta-Cell Mass and Body Weight Throughout the Lifespan in Lewis Rats. Diabetes 2000;49:1341–1346.

16. Kalra, M K, Maher, M M, Muller P R et al. State-of-the-art imaging of pancreatic neoplasms. Br. J. Radiol. 2003;76:857–865. doi: 10.1259/bjr/16642775.

17. Lu N, Feng X-Y, Hao S-J, Liang Z-H, Jin C, Qiang J-W, Guo Q-Y. 64-slice CT perfusion imaging of pancreatic adenocarcinoma and mass-forming chronic pancreatitis. Acad. Radiol. [Internet] 2011;18:81–8. doi: 10.1016/j.acra.2010.07.012.

18. Aime S, Caravan P. Biodistribution of gadolinium-based contrast agents, including gadolinium deposition. J. Magn. Reson. Imaging 2009;30:1259–67. doi: 10.1002/jmri.21969.

19. Lorusso V, Luzzani F, Bertani F, Tirone P, de Haën C. Pharmacokinetics and tissue distribution of iomeprol in animals. Eur. J. Radiol. 1994;18:S13–S20. doi: 10.1016/0720-048X(94)90090-6.

20. Cho HR, Choi SH. MR Imaging of the Pancreas in Streptozotocin-Induced Diabetic Rats: Comparison of Gadofluorine P and Gd-DOTA. In: World Molecular Imaging Society (WMIS). ; 2013. p. P544.

21. Gotthardt M, Lalyko G, van Eerd-Vismale J, et al. A new technique for in vivo imaging of specific GLP-1 binding sites: first results in small rodents. Regul. Pept. [Internet] 2006;137:162–7. doi: 10.1016/j.regpep.2006.07.005.

22. Grimm J, Potthast A, Wunder A, Moore A. Magnetic resonance imaging of the pancreas and pancreatic tumors in a mouse orthotopic model of human cancer. Int. J. Cancer [Internet] 2003;106:806–11. doi: 10.1002/ijc.11281.

23. Kalliokoski T, Svedström E, Roivainen A. Imaging of Insulitis in NOD Mice with IL-2-Gd-DTPA and 1.5 T MRI. Adv. Mol. Imaging 2011;01:43–49. doi: 10.4236/ami.2011.13006.

24. Wang P, Yoo B, Yang J, Zhang X, Ross A, Pantazopoulos P, Dai G, Moore A. GLP-1R-Targeting Magnetic Nanoparticles for Pancreatic Islet Imaging. Diabetes 2014;63:1465–74. doi: 10.2337/db13-1543.

Table 1 MR sequence parameters

	In Vivo		Post mortem		
Sequence	3D FLASH	SPACE	3D FLASH	SPACE	UTE
Matrix	256*256*160	256*256*160	256*256*144	256*256*144	176*176*176
Resolution (mm)	0.29*0.29*0.3	0.29*0.29*0.3	0.29*0.29*0.3	0.29*0.29*0.3	0.43*0.43*0.43
Bandwidth (Hz/pixel)	275	260	260	230	507
TE (ms)	3.69	144	3.69	132	0.07
TR (ms)	487.01	1500	13.74	1500	8.28
Fat saturation	-	-/+	-	-/+	-
Flip angles (degree)	10	variable	10	variable	15
Averages	1	2	1	1.4	1
GRAPPA	2	3	2	2	off
Phase Partial Fourier	off	67%	off	70%	off
Number of Phase Encoding Steps	256	176	256	183	36000
Scanning time	7 min	14 min	5 min 8 s	11 min 10 s	4 min 59 s

Table 2 Qualitative and quantitative image assessment

Objects	MRI *in vivo*/pre-	MRI post-	CT pre-	CT post-
		Contrast Ratio %		
Pancreas	NA	93.28 ± 34.61 %	NA	26.45 ± 5.29 %
		Visibility		
Pancreas	?/12	12/12	0/12	12/12
Splenic Vein	12/12	NA	0/12	0/12
CBD	12/12	NA	0/12	0/12

Note: pre-: precontrast; post-: postcontrast; NA: not applicable; ?: uncertain.

Figure legends:

Figure 1 Flowchart of experimental protocol. n: number of rats; CBD: common bile duct; MRI: magnetic resonance imaging; CT: computed tomography; Gadolodo-EB: Gd-DOTA, monomeric iodinated contrast agent Iomeprol and Evans blue solution.

Figure 2 Component chemical structures, vial outlook and HPLC UV-chromatogram of the mixed contrast medium dye solution Gadolodo-EB. On HPLC, Iomeprol first appeared at a retention time (RT) of 1.80±0.01 min and Evans blue dye came out with a RT of 5.99±0.02 min, identical to the respective RT when measured alone. The chemical structure of Gd-DOTA did not allow its detection by the applied HPLC method.

Figure 3 Coronal display of rat abdomen. **a&b:** *In vivo* T2 SPACE MRI for the common bile duct (CBD) and splenic vein. Hyperintense CBD and its distal extension of biliopancreatic duct (thick arrow) initiated from the hepatic hilum and extended to the gut (**a**), and hypointense splenic vein (thin arrow) merged into the portal vein (**b**). **c-d':** Postmortem MRI before and after Gadolodo-EB infusion. Pancreatic tissue could not be observed before contrast infusion on both T1 FLASH (**c**) and T2 SPACE (**c'**) images. Gd-DOTA in Gadolodo-EB solution induced contrast enhancement of the pancreas on T1 FLASH image (**d**), which corresponding to increased signal intensity on T2 SPACE image (**d'**) due to the long T2 water in the solvent. Hyperintense pancreatic region outline in FLASH image is delineated by green dashed line, the same outline is overlaid to SPACE image.

Figure 4 Pre- **(a, b)** and postcontrast **(a', b')** CT images: after Gadolodo-EB infusion , the pancreas was clearly shown in the middle of the abdomen on 2D image as indicated by arrows and in 3D rendering of postcontrast image. The granules (dashed circle) appeared on both pre- and postcontrast scans, indicative of calcified residuals of feces in the gut.

Figure 5 Three dimensional demonstration of postmortem T2 SPACE MRI with color coded orthoview of the pancreas (green) and fat distribution (purple) in rat abdomen at sagittal, coronal and transverse slice snaps: **a.** at the plane across pancreatic head, body and tail; **a'.** at the plane only across pancreatic head and tail. The surrounding topographic landmarks include stomach (St), caudate liver lobe (Cl), spleen (Sp),

right kidney (Rk), left kidney (Lk), and duodenum (Du). Arrows indicate fat tissue adjacent to the pancreas, which is otherwise difficult to distinguish.

Three dimensional rendering topography of the pancreas in rats using re-sampled CT to generate bony background scaffold: **b.** only the pancreas (green) was segmented and displayed due to Gadolodo-EB infusion; **b'.** organs surrounding the pancreas (green) were displayed to provide anatomic landmarks including the common bile duct (yellow), portal vein (blue), splenic vein (red), spleen (Sp, purple); stomach (St, bright grey), kidney (K, cabbage green), and guts (dark grey) with ascending colon (Ac), transverse colon (Tc) and descending colon (Dc).

Figure 6 Dissection and histology: **a.** digital photograph during autopsy displayed the pancreas as an Evans blue stained area adjacent to the stomach (St) and duodenum (Du); **b&c.** H&E stained microscopic view from Gadolodo-EB infused (b) and normal (c) pancreatic slices. Arrows indicate exocrine pancreatic tissues and arrowhead points to a pancreatic duct, and asterisks refer to islets of Langerhans. Scale bar: 50 μm.

Supplemental Digital Content 1 Video that demonstrates pre- and postcontrast CT images with 360° rotation.

Supplemental Digital Content 2 Video that rotationally demonstrates postcontrast MRI of segmented pancreas and surrounding topographic landmarks with precontrast CT bony thorax used as background scaffold. Refers to Fig. 5 for color coding.

Three-Dimensional Contrasted Visualization of Pancreas in Rats Using Clinical MRI and CT Scanners

Ting Yin, MSc[1]; Walter Coudyzer, MSc[2]; Ronald Peeters, PhD[2]; Yewei Liu, MD[1,3]; Marlein Miranda Cona, PhD[1]; Yuanbo Feng, MD, PhD[1,2]; Qian Xia, MD, PhD[1,3]; Jie Yu, MD[1,2]; Yansheng Jiang, PhD[1,2]; Steven Dymarkowski, MD, PhD[2]; Gang Huang, MD, PhD[3]; Feng Chen, MD, PhD[1,4]; Raymond Oyen, MD, PhD[2]; Yicheng Ni, MD, PhD[1,2*]

[1]Theragnostic Laboratory, Department of Imaging & Pathology, Biomedical Sciences Group, KU Leuven, Herestraat 49, 3000 Leuven, Belgium

[2]Department of Radiology, University Hospitals, KU Leuven, Herestraat 49, 3000 Leuven, Belgium

[3]Department of Nuclear Medicine, School of Medicine, Shanghai Jiaotong University, China

[4]Department of Radiology, the First Affiliated Hospital, Zhejiang University, China

[*]Corresponding author

Yicheng Ni MD, PhD

Department of Radiology, University Hospitals, KU Leuven, Herestraat 49, 3000 Leuven, Belgium

Email: yicheng.ni@med.kuleuven.be

Tel: +32 16 33 01 65

Fax: +32 16 34 37 65

Conflicts of interest and Source of Funding: The authors declare no conflict of interest. This study was partially supported by the grants awarded by the KU Leuven Molecular Small Animal Imaging Center MoSAIC (KUL EF/05/08) and KU Leuven the center of excellence In vivo Molecular Imaging Research (IMIR). The corresponding author Ni Y is currently a Bayer Lecture Chair holder.

Short title: Rat Pancreas on Contrasted MRI and CT

Abstract

Purpose: To visualize the pancreas in postmortem rats with local contrast medium infusion by three dimensional (3D) magnetic resonance imaging (MRI) and computed tomography (CT) using clinical imagers.

Methods: A total of 16 Sprague-Dawley rats about 300g were used for the pancreas visualization. Following the baseline imaging, a mixed contrast medium dye called Gadolodo-EB containing optimized concentrations of Gd-DOTA, Iomeprol and Evens blue was infused into the distally obstructed common bile duct (CBD) for postcontrast imaging at 3.0T MRI and 128-slice CT scanners. Images were post-processed with MeVisLab software package. MRI findings were co-registered with CT scans and validated with histomorphology, with relative contrast ratios quantified.

Results: Without contrast enhancement, the pancreas was indiscernible. After infusion of Gadolodo-EB solution, only pancreatic region became outstandingly visible, as shown by 3D rendering MRI and CT and proven by colored dissection and histological examinations. The measured volume of the pancreas averaged at 1.12±0.04cm^3 after standardization. Relative contrast ratios were 93.28±34.61% and 26.45±5.29% for MRI and CT respectively.

Conclusions: We have developed a multifunctional contrast medium dye to help clearly visualize and delineate rat pancreas *in situ* using clinical MRI and CT scanners. The topographic landmarks thus created with 3D demonstration may help to provide guidelines for the next *in vivo* pancreatic MR imaging research in rodents.

Key Words: contrast enhanced imaging, rat pancreas, image processing, 3D visualization

Introduction

Causative factors on the pancreas result in diseases such as pancreatitis, diabetes, and pancreatic tumors (1,2). The high incidence and mortality of pancreatic diseases have positioned imaging diagnosis a crucial place in daily clinical practice.

With the spatial and temporal resolution approaching that of computed tomography (CT), magnetic resonance imaging (MRI) has been increasingly utilized in clinic diagnosis of pancreatic lesions due to its additional advantages such as superb soft tissue contrast, ionizing-radiation free and multiparametric capacity (3,4). The combination of basic T1/T2 sequences, diffusion weighted imaging (DWI) and contrast enhanced MRI improves the accuracy of diagnosis for pancreatic tumors (5). The invention of MR cholangiopancreatography (MRCP) makes noninvasive examination of biliopancreatic duct system possible without any post-procedural complications (6,7).

In order to explore the mechanisms of pancreatic pathologies and develop new diagnostic and therapeutic techniques, rodent models are often used in pancreatic studies. However, unlike pancreas in humans, which is a retroperitoneal solid organ and can be identified by imaging even without contrast enhancement (3,8), rodent pancreas appears as an irregular lobulated organ, which is indiscernible compared to surrounding tissues, making imaging pancreas in rodents extremely challenging (9,10).

Efforts have been made in rodent pancreas MR imaging such as pancreatic islets imaging and pancreatic vessels permeability imaging using dynamic contrast enhanced MRI (11–13). However, due to the lack of pancreas specific labeling, pancreatic tissue in rodents itself is still very difficult to be distinguished from the surrounding structures such as caudate liver lobes, omenta and other peri-gastrointestinal soft tissues. Moreover, even after labeling, it is still challenging to have a complete overview of the entire pancreas due to the random movement of guts around pancreatic head portion. At this stage, the failure to image the entire pancreas has hampered our study on pancreatic diseases (e.g. acute pancreatitis), since nil or partial visualization of rodent pancreas could not reflect the overall pathological changes.

In this study, we intended to image rat pancreas *in situ* by using the state-of-the-art clinical MRI and CT scanners with the assistance of intra-pancreatic contrast enhancement. Detailed imaging landmarks and morphometry of rat pancreas were measured, described and presented with three dimensional (3D) rendering. Such postmortem investigation may help clearly recognize rat pancreas anatomy, provide a standard topography of this organ, and pave the way for the next *in vivo* 3D high resolution imaging studies on normal pancreas and pancreatic diseases in rat models.

Materials and methods

This experiment was approved by the ethical committee of our institute for animal research and welfare, and performed according to a designed protocol (Fig. 1).

Animals

Twelve Sprague-Dawley rats of equal genders weighing between 270 to 350g were subjected to both in vivo and postmortem imaging studies after being fasted for 6 hours prior to the experiments. Additional 4 rats of equal genders were used for dissection and histomorphological studies as normal controls.

Contrast solution preparation, characterization and administration

For multimodality contrasted imaging visualization of pancreas in rodents, phantoms with CT and MRI contrast agents at gradient concentrations and their dye mixtures were prepared and screened with CT and MRI. Consequently, a mixed hydrophilic solution called GadoIodo-EB containing 2 mM gadolinium contrast agent Gd-DOTA (Dotarem®, Guerbet, France) for MRI, Iomeprol (Iomeron®, Bracco, Italy) at 10 mg iodine/ml for CT and 0.1% Evans blue (EB, Sigma-Aldrich, USA) diluted in normal saline was optimized and made ready for instillation into the biliopancreatic duct at 0.6 ml per rat to demonstrate the pancreas by CT, MRI and visual inspection. Furthermore, such solutions of separate components or as a mixture GadoIodo-EB were characterized by high-performance liquid chromatography (UV-Vis HPLC detector 190-900 nm, Auckland, New Zealand) for testing their chemical stabilities.

In vivo MRI

MRI was performed at a 3.0T clinical scanner (Magnetom Tim Trio, Siemens, Erlangen, Germany). MR signal was transmitted through the 60 cm size bore body coil with maximum gradient amplitude of 45mT/m and slew rate of 200mT/m/ms, which was combined with an 8 channel phase array wrist coil as receiver. In vivo and postmortem MRI acquisition parameters are summarized in table 1. For in vivo MR scanning, animals were anesthetized by inhalation of 1 to 2 % isoflurane (mixed with oxygen and air) and placed in a supine position while images were acquired. MR compatible small animal physiological monitoring system (SAII, Stony Brook, NY, USA) was applied for respiration triggering. A 0.3 mm isotropic 3D gradient echo

flash low angle shot (FLASH) sequence with segmented k-space acquisition and a flow compensate T2 weighted 3D turbo spin-echo (TSE) with variable-flip-angle refocusing RF pulses (SPACE) sequence were performed.

Postmortem imaging acquisition

For preparing postmortem studies, rats were first anesthetized with intraperitoneal pentobarbital (Nembutal; Sanofi Sante Animale, Brussels, Belgium) at a dose of 40 mg/kg. After hair shaving and skin sterilization, a midline incision was made to expose the liver and other abdominal organs, particularly the hepatic portal area. To block the secretion pathway, the biliopancreatic duct was ligated in close vicinity to duodenal papilla, similarly to the technique mentioned in Kare's study (14). Afterwards, a 16 cm silicone catheter of 1.0 mm outer diameter (Degania Silicone Ltd, Degania Bet, 1513000, Israel) was inserted 6 mm deep into the common bile duct (CBD) near the hepatic port to the direction of duodenum for GadoIodo-EB infusion. The catheter was anchored with a 5-0 silk suture and connected to a 1.0 ml syringe loaded with the GadoIodo-EB contrast medium dye solution. After closure of abdominal incision by two layers of suture, the animal was euthanized by intravenous overdose of Nembutal to nullify imaging motion artifacts.

Following a baseline precontrast MRI scanning, pre- and postcontrast CT images were acquired on a clinic CT scanner (Somatom Definition Flash, Siemens, Erlangen, Germany) using low tube voltage of 80 kVp, total X-ray exposure time was 53s for each scan. High resolution transversal imaging was reconstructed and processed in Syngo CT 2012B with matrix size of 512*512, and a slice distance of 0.2 mm. Such 3D-CT scans allowed imaging rat abdomen on a relatively noise-free background to validate the presence of contrast agent in the pancreas (see video-supplement 1).

Postmortem MRI with 3D FLASH sequence was performed to evaluate the T1 enhancement by Gd-DOTA with isotropic spatial resolution of 0.3 mm, SPACE sequence was applied to acquire high-resolution anatomical information for rat abdomen, and ultra-short echo time (UTE) sequence was used to highlight tissues with short T2 in abdomen. Such 3D MRI scans enabled not only pancreas depiction but also neighboring organ localization (see video-supplement 2).

Image processing

All imaging analyses and visualizations were accomplished in MeVisLab platform (www.mevislab.de). CT images were co-registered to MRI space using MeVis Image Registration Toolkit (MERIT), in which affine transformation using normalized mutual information similarity measurements was applied. Afterwards, contrast enhanced pancreas was segmented from subtracted T1-weighted MR imaging and resampled CT imaging using fuzzy c-mean spatial classification algorithm with a proper intensity threshold, followed by region growing approach with 3D-6 nearest neighbor search. Segmented pancreas tissue volume was measured automatically.

Fat distribution in rat abdomen was delineated by subtracting SPACE scans with and without spectral fat saturation. Organs surrounding the pancreas were manually contoured or segmented semi-automatically from UTE or SPACE images only for 3D demonstration of pancreatic topography. Resampled pre-contrast CT bone image was used as background scaffold.

Tissue preparation and histology

After acquiring all images, animals were reopened to harvest the pancreas organ guided by Gadolodo-EB coloration. Dissection was made along the boundaries of the blue dye stained pancreatic tissues. The pancreas was cleaned from fat tissue and actual pancreatic volume was measured by immersing tissue into distilled water within a metering tank. Tissue was fixed in 10% formalin and embedded for paraffin sections. Afterwards, 5 μm thickness slices were stained with hematoxylin and eosin (HE) for optical microscopic assessment (Axioskop, Zeiss, Oberkoche, Germany) and digital photography to compare pancreatic tissues without and with contrast injection.

Image quality assessment

Signal intensity (SI) was measured within the pancreatic region, and contrast ratio (CR) after Gadolodo-EB infusion was calculated by the following equation: CR = [SI(post)-SI(pre)]/SI(pre)*100%. Visibility of the pancreas, splenic vein and CBD on both MRI and CT were assessed and summarized.

Results

General aspects

All experimental procedures were carried out smoothly according to the pre-designed protocol (Fig. 1) without accidental loss of animals. The clinical CT and MRI imagers were adapted well for the purpose of the present study in rats. No apparent variation of the pancreas was observed between male and female rats, although a movable kidney and an extra rib on the right were encountered in two individual rats as anatomical variations among this population.

Contrast agent solution characterization

A representative UV chromatogram of mixed contrast medium dye GadoIodo-EB consisting of 2.0 mM Gd-DOTA, 10mg Iodine/ml Iomeprol and 0.1% Evans blue dye is shown in Figure 2. The profiles clearly revealed only two peaks whose retention times (RTs) perfectly matched with those observed by analyzing separate standard solutions of Iomeprol and Evans blue dye (data not shown). The sharp peak corresponded to the CT agent Iomeprol with a RT of 1.80±0.01 min. The second broad peak with a RT of 5.99±0.02 min referred to Evans blue. Neither in the standard solution nor in the mixture of Gadolodo-EB could Gd-DOTA be detected due to its structural lack of UV chromospheres for the HPLC technique applied. However, both peaks of Iomeprol and Evans blue in the mixture were not altered by adding Gd-DOTA, of which the presence was affirmed by the MRI studies, indicating that no chemical reactions occurred within the mixture of Gadolodo-EB. Phantom studies showed that neither the presence of Gd-DOTA on CT nor Iomeprol on MRI changed intrinsic signal intensity of the contrast medium dye at their concentrations applied.

In vivo MRI

Three dimensional high resolution in vivo MRI without contrast enhancement displayed abdominal anatomy that could be useful for searching pancreas-related landmarks such as the CBD or biliopancreatic duct and splenic vein. For examples, on 3D T2 SPACE image, the CBD and its extending biliopancreatic duct appeared with a strong hyperintensity (Fig. 3a, table 2) and hypointense splenic vein was

shown in full length, which likely goes along with pancreatic body and tail (Fig. 3b, table 2), as revealed by later contrasted postmortem studies.

Contrast enhanced MRI

Pre- and postcontrast T1 and T2 MRI images are shown with the same anatomic positions. On T1 FLASH image, before contrast infusion, there was no difference of signal intensities between the pancreas and surrounding organs (Fig. 3c, table 2). After GadoIodo-EB infusion, pancreatic region appeared hyperintense, indicating the T1-shortening effect of the gadolinium chelate (Fig. 3d, table 2). On T2 SPACE images, the pancreas was virtually invisible (Fig. 3c'). But, hyperintense signal intensity appeared after GadoIodo-EB infusion due to the presence of saline solvent or long-T2 water (Fig. 3d'), because the low-concentrated Gd-DOTA had negligible T2--shortening effects.

CT findings

Before contrast instillation, the pancreas was invisible when image density was set to a threshold value for bone visualization by experienced radiologists (Fig. 4a, 4b). But, the infused GadoIodo-EB provided a clear contrast for pancreas alone, displaying it as an outstanding organ in abdomen (Fig. 4a', b'). In addition to the pancreas, hyperdense subjects also existed in the abdominal region on pre-contrast CT scan, which were proven as calcified food residues within the fecal pellets located in large intestines (Fig. 4b, b' and video supplements).

Topographic descriptions

As shown by postmortem contrasted CT and MRI scans in this study (Fig. 3-5), the entire pancreas in rats appears as a "T" shaped structure, but tilted 90° to the right, with the short vertical bar (pancreatic head) at least 2 times thicker than the long horizontal bar (pancreatic body and tail). The entire rat pancreas locates in the upper abdomen at the level either between the 11^{th} thoracic vertebra (T11) and the 2^{nd} lumbar vertebra (L2) or between the T12 and L3 with slight individual variations (Fig. 5b, b' and video supplements). Similar to that of humans, though not in the same proportions, the pancreas in rats can be divided into pancreatic head, body and tail. The head is further divided into the biliary portion located along the CBD on the right side of portal vein and gastric pylorus, and the duodenal portion largely enclosed by

the “C” shaped duodenum to the left of the right kidney. The pancreatic body and tail form a horizontal entity that is also called gastrosplenic portion located inferior to the stomach to the right of the spleen (14) and left kidney (video supplements).

Contrasted topography of rat pancreas imaging enabled recognizing a few landmarks that may help position the pancreas in rats *in vivo* as described below:

1) a 2-cm elongation line from the CBD downwards can be referred as a landmark for localizing pancreatic head anterior to the hilum of the right kidney and largely wrapped by the duodenal loop (Fig. 3a, 5b’);

2) pancreatic body and tail locate inferoposterior to the stomach and caudate lobes of the liver and adjacent to the anterosuperior part of the left kidney (Fig. 5a, a’);

3) the entire splenic vein joining to the portal vein goes along with pancreatic body and tail to the right of the spleen and in front of the left kidney (Fig. 3b, c, c’).

Their relative positions are illustrated by color-coded imaging extraction (Fig. 5b’). Fat tissues can be confused with the pancreas, which could be differentiated by highlighting the fat (in purple color) using fat saturated SPACE images (Fig. 5a, a’). Segmented pancreas and its landmarks were shown by 3D rending images using the bony thorax as a background scaffold (Fig. 5b, b’ and video supplement 2).

Dissection and histology

Under a re-laparotomy for *ex vivo* examinations, digital photos showed Evans blue staining of pancreatic tissues (Fig. 6a). Microscopically, pancreatic exocrine tissue, expanded pancreatic duct and endocrine islets of Langerhans were identified with H&E stained histology. Except slightly dilated exocrine glandular system, there was no significant difference between contrast-infused and control pancreases (Fig. 6b, c).

Quantitative measurements

After adjusted normalization, pancreatic volumes measured by imaging and *ex vivo* analysis were 1.12 ± 0.04 cm^3 and 1.17 ± 0.10 cm^3 respectively, which is in line with the pancreas weight about 1.2 g for SD rats ranging from 270 to 450 g of body weight as reported by a previous study (15). The relative contrast ratio for post-contrast FLASH-MRI and CT images was enhanced by 93.28 ± 34.61 % and 26.45 ± 5.29 % respectively compared to pre-contrast images (table 2).

Discussion

One bottleneck of research on pancreatic disorders in rodents is the virtual inability to noninvasively detect the lesion on this organ, to monitor the disease progress and to follow up the therapies by imaging modalities, which has hampered advances in the field. As the first step in our serial efforts, we attempted to visualize rat pancreas postmortem by contrast enhanced MRI and CT using clinically available imagers. To the best of our knowledge, it is the first time that the in situ rodent pancreas is so clearly depicted in terms of its location, dimension, contour and relations to the adjacent anatomical structures, which may provide useful clues or landmarks for identifying rat pancreas and its pathologies during further in vivo pancreatic imaging research.

Currently, CT is still the most commonly used imaging modality for diagnosis of pancreatitis and pancreatic tumors due to its temporal efficiency and unbiased contrast compared to MRI (16,17). Therefore, we applied CT for cross-reference to our MRI findings.

The utilization of the clinical MRI and CT scanners in combination with the FDA approved contrast agents would make our findings more clinically translational. It also demonstrates that clinicians in academic institutes could perform preclinical animal experiments without relying on the dedicated equipment for small animals. Since the achievable spatial resolution could be limited in comparison to the miniaturized animal imagers, certain technical optimization was necessary particularly for imaging rat pancreas as a tiny irregular abdominal organ.

Accordingly, we adapted higher resolution 3D scanning protocols to include as many details as possible, though such 3D scans were more time-consuming with higher imaging noise relative to 2D scans. In this study, both T1 weighted FLASH and T2 weighted SPACE protocols were applied for contrasted and structural evaluations respectively. Results showed that without regional contrast agent instillation, it was impossible to distinguish rodent pancreas from the surrounding tissues through those imaging protocols.

Because a real pancreas-specific contrast agent does not exist, in this study we prepared a mixed water-soluble solution GadoIodo-EB that consists of two extracellular water-soluble contrast agents, Gd-DOTA for MRI and Iomeprol for CT

(18,19) both of which do not undergo intracellular uptake, and a blue dye. Once infused, the solution with optimized concentrations of gadolinium and iodine was filled into the exocrine glandular system, leading to the striking contrast observed only in the pancreas on both MRI and CT scans. The postcontrast inhomogeneity of MRI signal within the pancreas reflects such intraorganal distribution pattern of Gd-DOTA as also evidenced on colored dissection. The mixture of these two contrast agents with Evans blue dye did not alter their chemical properties as proven by HPLC. Since all these 3 components are nontoxic and intravenously injectable in humans, and since imaging and HPLC outcomes in our study have implied their inert chemical properties while mixed, GadoIodo-EB as a multifunctional diagnostic agent could be combined with interventional procedures e.g. endoscopic retrograde cholangiopancreatography (ERCP) and laparoscopic cholecystectomy, etc. for multimodality imaging diagnosis and/or intraoperative optical imaging observation. Such potential clinical applications warrant further experimental investigations.

Without local contrast instillation, the pancreas shows the same signal intensity or tissue density as the liver does. Thus hepatic caudate lobe, which locates closely next to the pancreatic body, could be mistaken as the pancreas in the literature (20). Indeed, the pancreas shares similar soft tissue imaging features with other abdominal organs on both MRI and CT, even after systematical contrast agent administration. Therefore, it is essential to track the pancreas in vivo by carefully navigating through certain landmarks including adjacent organs and important vessels on 3D images. Thus, guided by the artificially contrasted pancreas in this study, we were able to identify a few such useful landmarks including the CBD, splenic vein, caudate liver lobes, the stomach, the duodenum, the right and left kidney and the spleen, which together make the in-between contour of pancreas. Abdominal fat tissues in rats especially those adhered to the pancreas could be distinguished by using fat-saturation MRI sequences. However, omentum tissues appeared more difficult to identify, which could only be recognized on histology.

MRI is known to be superior to CT in soft tissue contrast, but the plain scans of both modalities proved insufficient to visualize rodent pancreas, and the use of contrast agents was deemed necessary. For this, two obstacles should be tackled. First, since pancreas-specific contrast agents do not exist, we had to use commercially available nonspecific ones such as Gd-DOTA and Iomeprol for MRI and CT respectively. They

are made for intravenous injection at a high concentration. After administration they undergo extracellular distribution without intracellular uptake, and tissues or organs are properly enhanced by them at much diluted concentrations. If without dilution, the presence of CT or MRI contrast agents at their original concentrations (0.5M for Gd-DOTA and 300mg Iodine/ml for Iomeprol) in the scanned volume would cause strong artifacts that would mask the authentic images. This was the reason why we had to perform in vitro tests first to optimize the mixed contrast dye Gadolodo-EB for the appropriate concentrations of both Gd-DOTA and Iomeprol. Secondly, the presence of such a contrast dye had to be confined only in the pancreas but not elsewhere to selectively enhance this organ on both CT and MR images. To do so, we took advantage of the biliopancreatic anatomy in rats and filled the pancreatic exocrine ductal system entirely with Gadolodo-EB so that only the pancreas could be outstandingly enhanced on both CT and MRI.

In order to avoid blooming effect while maintaining adequate contrast enhancement, the concentration of each contrast agent used in this study was optimized to a clinically acceptable range. The total volume of Gadolodo-EB for infusion into the pancreas was also controlled to less than the total volume of pancreas.

There were rodent pancreatic imaging using micro-CT (9), and specific pancreatic labeling using high-resolution SPECT technique (21). Contrast enhanced MRI suffered from motion artifact due to the special location of pancreas (22). As observed by both imaging and histology, pancreatic head was closely surrounded by duodenum and attached to the large intestine, where the wave movement was unpredictable and cannot be monitored, which leads to blurring artifact of the entire region. Therefore, fasting is preferred prior to in vivo imaging to reduce gut movements. Besides, fasting for 6 hours leaves more upper abdominal space for Gadolodo-EB infusion and eases surgical operation. More specific enhancement on inflamed pancreas (23) or pancreatic islets surface reporter (24) may help improve the imaging accuracy on the pancreas, however such specific contrast agents are still unavailable.

From our in vivo observations, without contrast enhancement, the CBD showed prominent hyperintense on SPACE images. Pancreatic ducts, on the other hand, were difficult to highlight due to the limited spatial resolution. Although there are

abundant blood supplies to the pancreas, only the splenic vein was thick enough to be observed by our imaging sequences. Therefore, it seems also essential for in vivo pancreas imaging to apply a contrast agent, ideally a pancreas-specific one.

In conclusion, visualization of a complete pancreas was achieved through contrast enhanced CT and MRI imaging in a novel rat postmortem model. Detailed pancreatic landmarks were thus described and demonstrated with 3D rendering, including the depicted CBD and splenic vein on in vivo images. To identify other in vivo features of rodent pancreas, contrast enhanced protocols will be elaborated in the future.

References

1. Nakamura T, Takeuchi T, Tando Y. Pancreatic dysfunction and treatment options. Pancreas 1998;16:329–36.

2. Cascinu S, Falconi M, Valentini V, Jelic S. Pancreatic cancer: ESMO Clinical Practice Guidelines for diagnosis, treatment and follow-up. Ann. Oncol. 2010;21:55–58. doi: 10.1093/annonc/mdq165.

3. Sandrasegaran K, Lin C, Akisik FM, Tann M. State-of-the-art pancreatic MRI. Am. J. Roentgenol. 2010;195:42–53. doi: 10.2214/ajr.195.3_supplement.0s42.

4. Chaudhary V, Bano S. Imaging of the pancreas: Recent advances. Indian J. Endocrinol. Metab. 2011;15:S25–32. doi: 10.4103/2230-8210.83060.

5. Schima W. MRI of the pancreas: tumours and tumour-simulating processes. Cancer Imaging 2006;6:199–203. doi: 10.1102/1470-7330.2006.0035.

6. Fulcher AS, Turner MA. MR pancreatography: a useful tool for evaluating pancreatic disorders. Radiographics 1998;19:5–24. doi: 10.1148/radiographics.19.1.g99ja045.

7. Nandalur KR, Hussain HK, Weadock WJ, Wamsteker EJ, Johnson TD, Khan AS, D'Amico AR, Ford MK, Nandalur SR, Chenevert TL. Possible biliary disease: diagnostic performance of high-spatial-resolution isotropic 3D T2-weighted MRCP. Radiology 2008;249:883–90. doi: 10.1148/radiol.2493080389.

8. Sainani N, Catalano O, Sahani D. Pancreas. In: John R. Haaga, Vikram S. Dogra, Michael Forsting E, editor. CT and MRI of the Whole Body. 5th ed. Elsevier; 2002.

9. Akladios CY, Bour G, Raykov Z, Mutter D, Marescaux J AM. Structural imaging of the pancreas in rat using micro-CT: application to a non-invasive longitudinal evaluation of pancreatic ductal carcinoma monitoring. J Cancer Res Ther 2013;1:70–76.

10. Tchokonte-Nana V, Longo-Mbenza B, Page BJ, Du Toit DF. Morphogenetic and clinical perspectives on the neogenesis of pancreatic duct ligation-induced islet cells : a review. Adv Clin Exp Med [Internet] 2011;20:5–14.

11. Lamprianou S, Immonen R, Nabuurs C, Gjinovci A, Vinet L, Montet XCR, Gruetter R, Meda P. High-resolution magnetic resonance imaging quantitatively detects individual pancreatic islets. Diabetes 2011;60:2853–60. doi: 10.2337/db11-0726.

12. Medarova Z, Greiner DL, Ifediba M, Dai G, Bolotin E, Castillo G, Bogdanov A, Kumar M, Moore A. Imaging the pancreatic vasculature in diabetes models. Diabetes. Metab. Res. Rev. 2011;27:767–72. doi: 10.1002/dmrr.1249.

13. Medarova Z, Castillo G, Dai G, Bolotin E, Bogdanov A, Moore A. Noninvasive magnetic resonance imaging of microvascular changes in type 1 diabetes. Diabetes 2007;56:2677–82. doi: 10.2337/db07-0822.

14. Kara ME. The anatomical study on the rat pancreas and its ducts with emphasis on the surgical approach. Ann. Anat. 2005;187:105–12. doi: 10.1016/j.aanat.2004.10.004.

15. Montanya E, Nacher V, Soler, Joan E. Linear Correlation Between beta-Cell Mass and Body Weight Throughout the Lifespan in Lewis Rats. Diabetes 2000;49:1341–1346.

16. Kalra, M K, Maher, M M, Muller P R et al. State-of-the-art imaging of pancreatic neoplasms. Br. J. Radiol. 2003;76:857–865. doi: 10.1259/bjr/16642775.

17. Lu N, Feng X-Y, Hao S-J, Liang Z-H, Jin C, Qiang J-W, Guo Q-Y. 64-slice CT perfusion imaging of pancreatic adenocarcinoma and mass-forming chronic pancreatitis. Acad. Radiol. [Internet] 2011;18:81–8. doi: 10.1016/j.acra.2010.07.012.

18. Aime S, Caravan P. Biodistribution of gadolinium-based contrast agents, including gadolinium deposition. J. Magn. Reson. Imaging 2009;30:1259–67. doi: 10.1002/jmri.21969.

19. Lorusso V, Luzzani F, Bertani F, Tirone P, de Haën C. Pharmacokinetics and tissue distribution of iomeprol in animals. Eur. J. Radiol. 1994;18:S13–S20. doi: 10.1016/0720-048X(94)90090-6.

20. Cho HR, Choi SH. MR Imaging of the Pancreas in Streptozotocin-Induced Diabetic Rats: Comparison of Gadofluorine P and Gd-DOTA. In: World Molecular Imaging Society (WMIS). ; 2013. p. P544.

21. Gotthardt M, Lalyko G, van Eerd-Vismale J, et al. A new technique for in vivo imaging of specific GLP-1 binding sites: first results in small rodents. Regul. Pept. [Internet] 2006;137:162–7. doi: 10.1016/j.regpep.2006.07.005.

22. Grimm J, Potthast A, Wunder A, Moore A. Magnetic resonance imaging of the pancreas and pancreatic tumors in a mouse orthotopic model of human cancer. Int. J. Cancer [Internet] 2003;106:806–11. doi: 10.1002/ijc.11281.

23. Kalliokoski T, Svedström E, Roivainen A. Imaging of Insulitis in NOD Mice with IL-2-Gd-DTPA and 1.5 T MRI. Adv. Mol. Imaging 2011;01:43–49. doi: 10.4236/ami.2011.13006.

24. Wang P, Yoo B, Yang J, Zhang X, Ross A, Pantazopoulos P, Dai G, Moore A. GLP-1R-Targeting Magnetic Nanoparticles for Pancreatic Islet Imaging. Diabetes 2014;63:1465–74. doi: 10.2337/db13-1543.

Table 1 MR sequence parameters

	In Vivo		Post mortem		
Sequence	3D FLASH	SPACE	3D FLASH	SPACE	UTE
Matrix	256*256*160	256*256*160	256*256*144	256*256*144	176*176*176
Resolution (mm)	0.29*0.29*0.3	0.29*0.29*0.3	0.29*0.29*0.3	0.29*0.29*0.3	0.43*0.43*0.43
Bandwidth (Hz/pixel)	275	260	260	230	507
TE (ms)	3.69	144	3.69	132	0.07
TR (ms)	487.01	1500	13.74	1500	8.28
Fat saturation	-	-/+	-	-/+	-
Flip angles (degree)	10	variable	10	variable	15
Averages	1	2	1	1.4	1
GRAPPA	2	3	2	2	off
Phase Partial Fourier	off	67%	off	70%	off
Number of Phase Encoding Steps	256	176	256	183	36000
Scanning time	7 min	14 min	5 min 8 s	11 min 10 s	4 min 59 s

Table 2 Qualitative and quantitative image assessment

Objects	MRI *in vivo*/pre-	MRI post-	CT pre-	CT post-
		Contrast Ratio %		
Pancreas	NA	93.28 ± 34.61 %	NA	26.45 ± 5.29 %
		Visibility		
Pancreas	?/12	12/12	0/12	12/12
Splenic Vein	12/12	NA	0/12	0/12
CBD	12/12	NA	0/12	0/12

Note: pre-: precontrast; post-: postcontrast; NA: not applicable; ?: uncertain.

Figure legends:

Figure 1 Flowchart of experimental protocol. n: number of rats; CBD: common bile duct; MRI: magnetic resonance imaging; CT: computed tomography; Gadolodo-EB: Gd-DOTA, monomeric iodinated contrast agent Iomeprol and Evans blue solution.

Figure 2 Component chemical structures, vial outlook and HPLC UV-chromatogram of the mixed contrast medium dye solution Gadolodo-EB. On HPLC, Iomeprol first appeared at a retention time (RT) of 1.80±0.01 min and Evans blue dye came out with a RT of 5.99±0.02 min, identical to the respective RT when measured alone. The chemical structure of Gd-DOTA did not allow its detection by the applied HPLC method.

Figure 3 Coronal display of rat abdomen. **a&b:** *In vivo* T2 SPACE MRI for the common bile duct (CBD) and splenic vein. Hyperintense CBD and its distal extension of biliopancreatic duct (thick arrow) initiated from the hepatic hilum and extended to the gut (**a**), and hypointense splenic vein (thin arrow) merged into the portal vein (**b**). **c-d':** Postmortem MRI before and after Gadolodo-EB infusion. Pancreatic tissue could not be observed before contrast infusion on both T1 FLASH (**c**) and T2 SPACE (**c'**) images. Gd-DOTA in Gadolodo-EB solution induced contrast enhancement of the pancreas on T1 FLASH image (**d**), which corresponding to increased signal intensity on T2 SPACE image (**d'**) due to the long T2 water in the solvent. Hyperintense pancreatic region outline in FLASH image is delineated by green dashed line, the same outline is overlaid to SPACE image.

Figure 4 Pre- **(a, b)** and postcontrast **(a', b')** CT images: after Gadolodo-EB infusion , the pancreas was clearly shown in the middle of the abdomen on 2D image as indicated by arrows and in 3D rendering of postcontrast image. The granules (dashed circle) appeared on both pre- and postcontrast scans, indicative of calcified residuals of feces in the gut.

Figure 5 Three dimensional demonstration of postmortem T2 SPACE MRI with color coded orthoview of the pancreas (green) and fat distribution (purple) in rat abdomen at sagittal, coronal and transverse slice snaps: **a.** at the plane across pancreatic head, body and tail; **a'.** at the plane only across pancreatic head and tail. The surrounding topographic landmarks include stomach (St), caudate liver lobe (Cl), spleen (Sp),

right kidney (Rk), left kidney (Lk), and duodenum (Du). Arrows indicate fat tissue adjacent to the pancreas, which is otherwise difficult to distinguish.

Three dimensional rendering topography of the pancreas in rats using re-sampled CT to generate bony background scaffold: **b.** only the pancreas (green) was segmented and displayed due to Gadolodo-EB infusion; **b'.** organs surrounding the pancreas (green) were displayed to provide anatomic landmarks including the common bile duct (yellow), portal vein (blue), splenic vein (red), spleen (Sp, purple); stomach (St, bright grey), kidney (K, cabbage green), and guts (dark grey) with ascending colon (Ac), transverse colon (Tc) and descending colon (Dc).

Figure 6 Dissection and histology: **a.** digital photograph during autopsy displayed the pancreas as an Evans blue stained area adjacent to the stomach (St) and duodenum (Du); **b&c.** H&E stained microscopic view from Gadolodo-EB infused (b) and normal (c) pancreatic slices. Arrows indicate exocrine pancreatic tissues and arrowhead points to a pancreatic duct, and asterisks refer to islets of Langerhans. Scale bar: 50 μm.

Supplemental Digital Content 1 Video that demonstrates pre- and postcontrast CT images with 360° rotation.

Supplemental Digital Content 2 Video that rotationally demonstrates postcontrast MRI of segmented pancreas and surrounding topographic landmarks with precontrast CT bony thorax used as background scaffold. Refers to Fig. 5 for color coding.

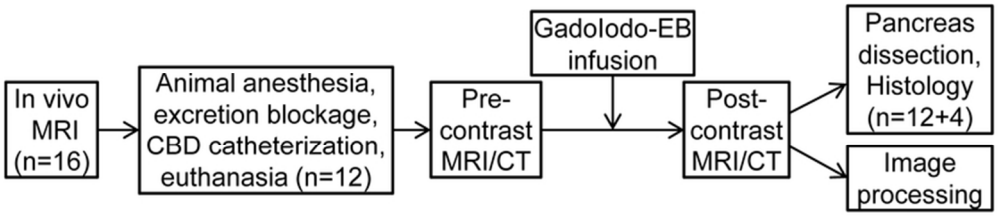

Figure 1
35x7mm (600 x 600 DPI)

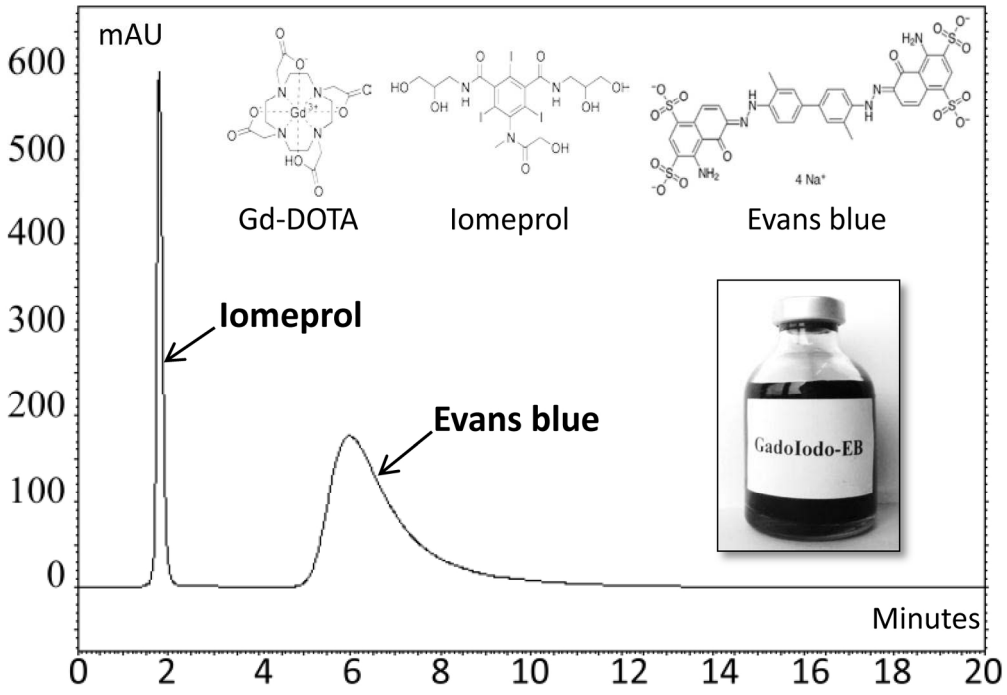

Figure 2
89x61mm (600 x 600 DPI)

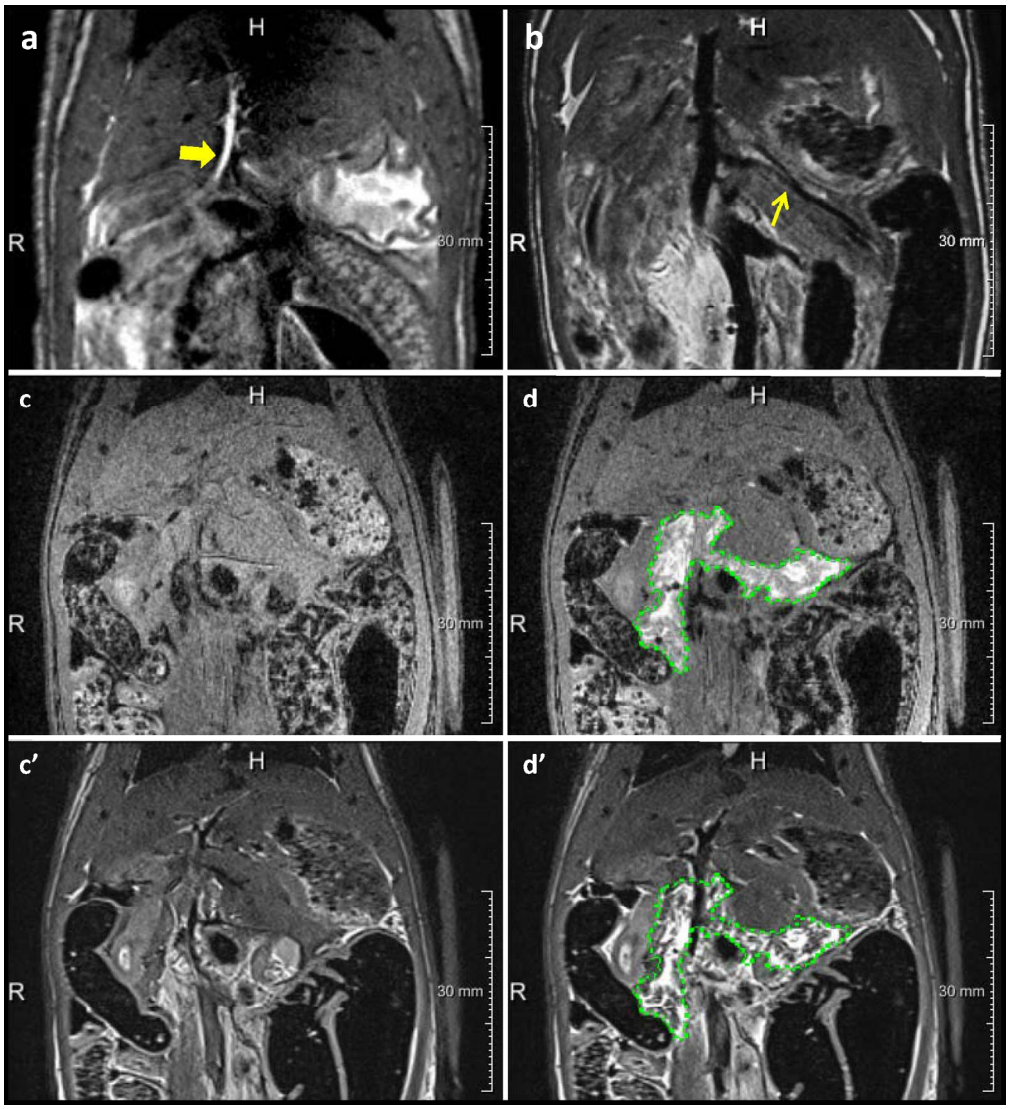

Figure 3
169x185mm (300 x 300 DPI)

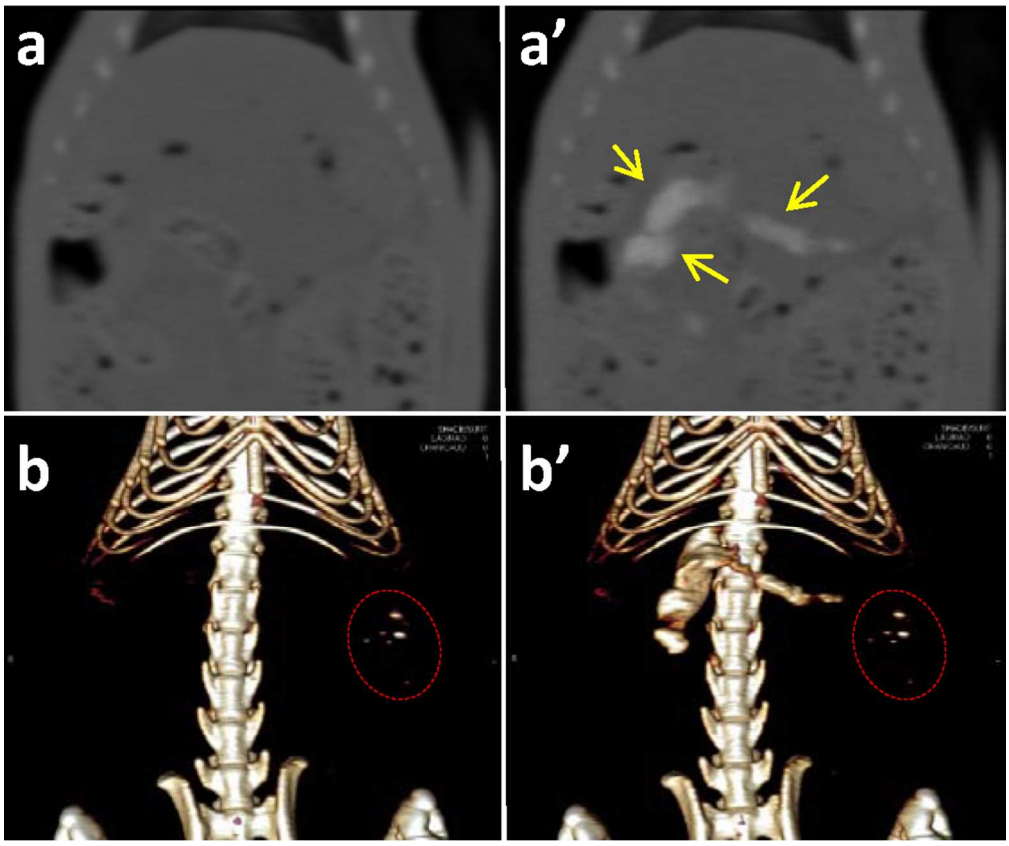

Figure 4
94x79mm (300 x 300 DPI)

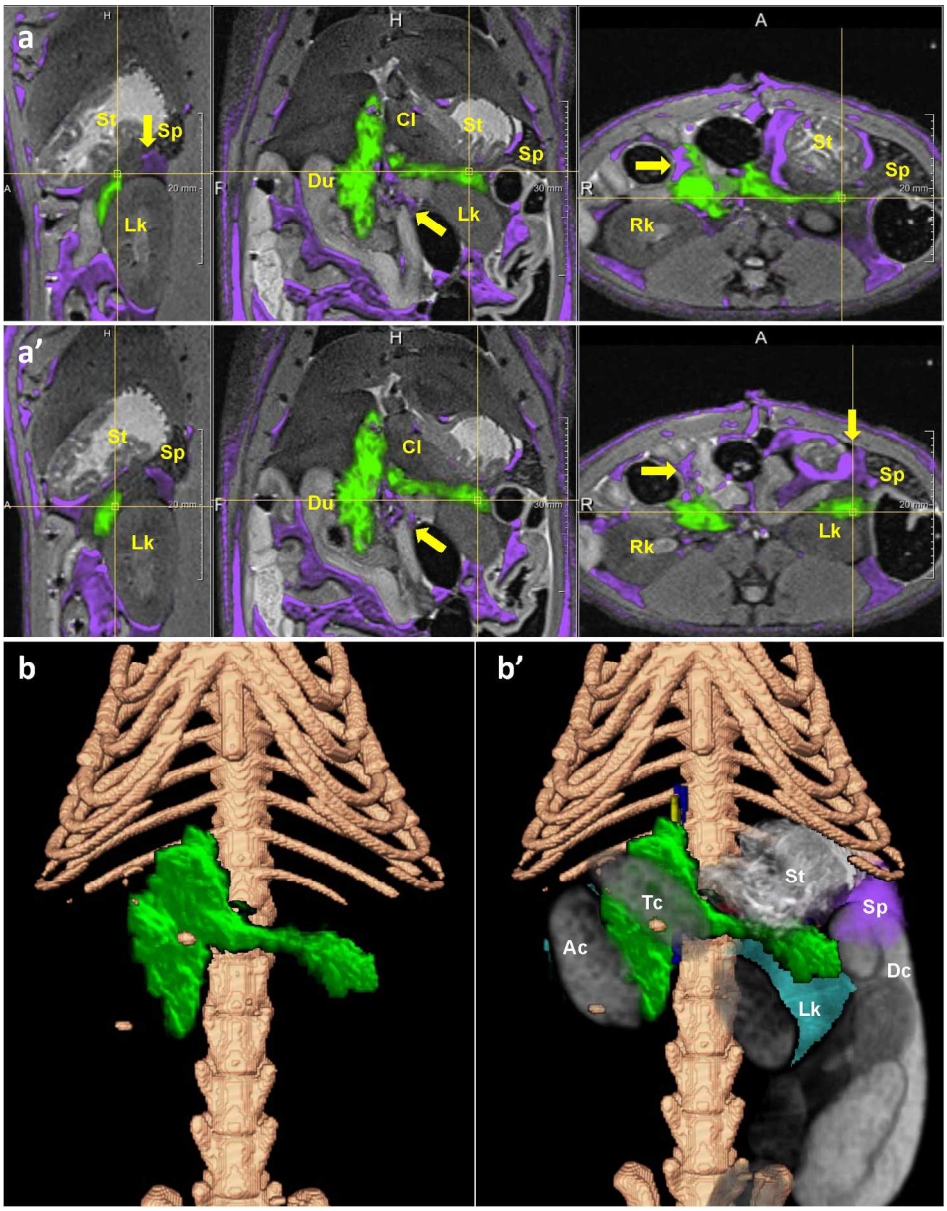

Figure 5
169x216mm (300 x 300 DPI)

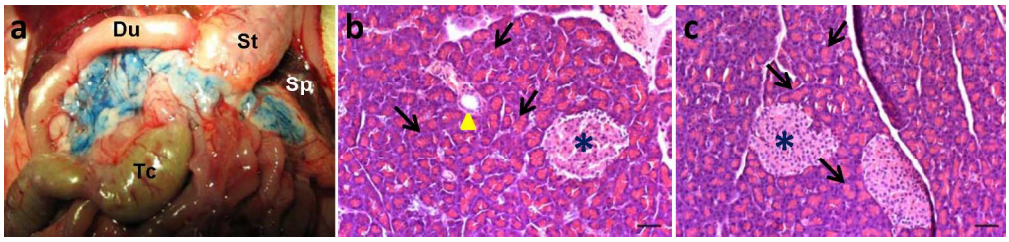

Figure 6
171x39mm (300 x 300 DPI)